J. Embryol. exp. Morph. 98, 1–19 (1986)
Printed in Great Britain © The Company of Biologists Limited 1986

Transformation of a polygonal cellular pattern during sexual maturation of the avian oviduct epithelium: computer simulation

HISAO HONDA, HACHIRO YAMANAKA
Kanebo Institute for Cancer Research, Tomobuchicho 1-5-90, Osaka 534 Japan
AND GORO EGUCHI
National Institute for Basic Biology, Okazaki 444 Japan

SUMMARY

A peculiar cellular pattern resembling a checkerboard has been observed on the luminal surface of the oviduct epithelium of an adult Japanese quail. The epithelium is a monolayer cell sheet and consists of two types of columnar cells, ciliated cells (C-cells) and gland cells (G-cells) assembled in alternating blocks. The pattern develops, during sexual maturation, from a kagome-like pattern (in which large C-cells are surrounded by small G-cells) characteristic of the immature oviduct. In the present paper, computer simulations of the pattern transformation from kagome to checkerboard were performed assuming a few properties of individual cells.

The adult checkerboard-like pattern is not strictly rectangular, but is deformed toward a honeycomb pattern. In theoretical considerations the assumption that adhesion is stronger between unlike cells than between like cells formed an ideal checkerboard pattern, because all cell boundaries in it are edges along which unlike cells meet. On the other hand, a honeycomb pattern formed after assuming that the boundary length of the cellular pattern is minimized (caused by contraction of bundles of microfilaments running along lateral boundaries of the columnar epithelial cell while keeping contact between neighbouring cells). The actual checkerboard-like pattern was considered to be in a balanced state between the effects of (1) the strong adhesion between unlike cells, and (2) the boundary contraction. Using a computational analysis, this consideration enabled us to obtain a quantitative parameter value for the difference between cell adhesions of unlike cells and of like cells.

C-cells divided once during the kagome–checkerboard transformation, while G-cells did not divide. We performed computer simulations starting with the kagome pattern in which all C-cells divided once. The computer program of the boundary shortening procedure we used involved the quantitative parameter value for differential cell adhesion obtained as described above. A checkerboard pattern was successfully generated in the simulation. It is concluded that the strong adhesion between unlike cells and the boundary shortening have important roles in formation and maintenance of the kagome and checkerboard patterns of the avian oviduct epithelium.

INTRODUCTION

In previous papers we constructed a boundary contracting cell model based on an observation of bundles of microfilaments running along lateral boundaries of epithelial cells (Honda & Eguchi, 1980; Honda, 1983). The model was used to

Key words: cell boundary contraction, cellular pattern, checkerboard pattern, computer simulation, differential cell adhesion, kagome pattern, oviduct epithelium, avian oviduct.

investigate an epithelial cellular pattern and to distinguish an epithelial tissue from others in a homogeneous cell system (Honda, Ogita, Higuchi & Kani, 1982; Honda, Dan-Sohkawa & Watanabe, 1983).

Recently, we discovered peculiar cellular patterns in a heterogeneous cell system of the epithelium. The luminal surface of an avian oviduct epithelium consisting of two types of cells shows a kagome (or star) pattern when immature (Fig. 1A,C: large cells are surrounded by small cells) and a checkerboard pattern in the mature state (Fig. 1B,D: two types of cells are arranged alternately). Observation of the oviduct epithelium is described in detail elsewhere (Yamanaka & Honda, in preparation; Yamanaka, in preparation). There we preliminarily use the concept of differential cell adhesion in order to understand the formation of these peculiar patterns. Assuming that unlike cells adhere to each other more strongly than like cells cohere, we can explain the formation of kagome and checkerboard patterns. We speculate that the actual oviduct epithelium is governed by two simultaneous factors, boundary contraction and differential cell adhesions.

In the present paper the relation between the two factors is considered in detail and the transformation of the kagome pattern into the checkerboard pattern during development, which involves cell divisions, is simulated successfully by computer using assumptions about cell behaviours due to these two factors.

MATERIALS AND METHODS

Oviduct

Eggs of the Japanese quail (*Coturnix coturnix japonica*) were hatched in the laboratory. Oviducts were isolated from dead female animals at desired maturation stages and treated with silver nitrate to facilitate observation of the cell boundaries (Yamanaka, in preparation). Luminal surfaces of the magnum of the oviduct were observed throughout the present study.

Improvement of the usual cell model

We used a model for the shortening of intercellular boundaries in order to determine whether a given cell sheet had the geometrical characteristics of an epithelium and to convert a polygonal pattern of the given cell sheet into the expected pattern for an epithelium in which cell boundaries had shortened. Detailed procedures are described elsewhere (Honda & Eguchi, 1980; Honda, 1983; Honda, Dan-Sohkawa & Watanabe, 1983). The boundary shortening model was improved in order to apply it to a heterogeneous cell system and to move cell boundaries smoothly in the computer simulation. A total standard procedure is summarized in Fig. 2.

(1) *For a heterogeneous system*

We considered a polygonal cellular pattern that was the surface view of a cell monolayer. Two arbitrary vertices (P and Q in Fig. 3) linked by a side were chosen in a given polygonal pattern and they were moved so as to maintain a constant area for each polygon as shown in Fig. 3. The 'weighted' length of the five sides was defined as

$$a_{AP}AP' + a_{BP}BP' + a_{PQ}P'Q' + a_{QC}Q'C + a_{QD}Q'D\,,$$

which was calculated from the position P′ (which moved along the line containing P and was parallel with AB). The values of the weighting factors, $a_{AP}, a_{BP}, a_{PQ}, \ldots$ depended on the types of cells meeting at the boundaries, AP, BP, PQ, ... As there are two types of cells, C (ciliated)

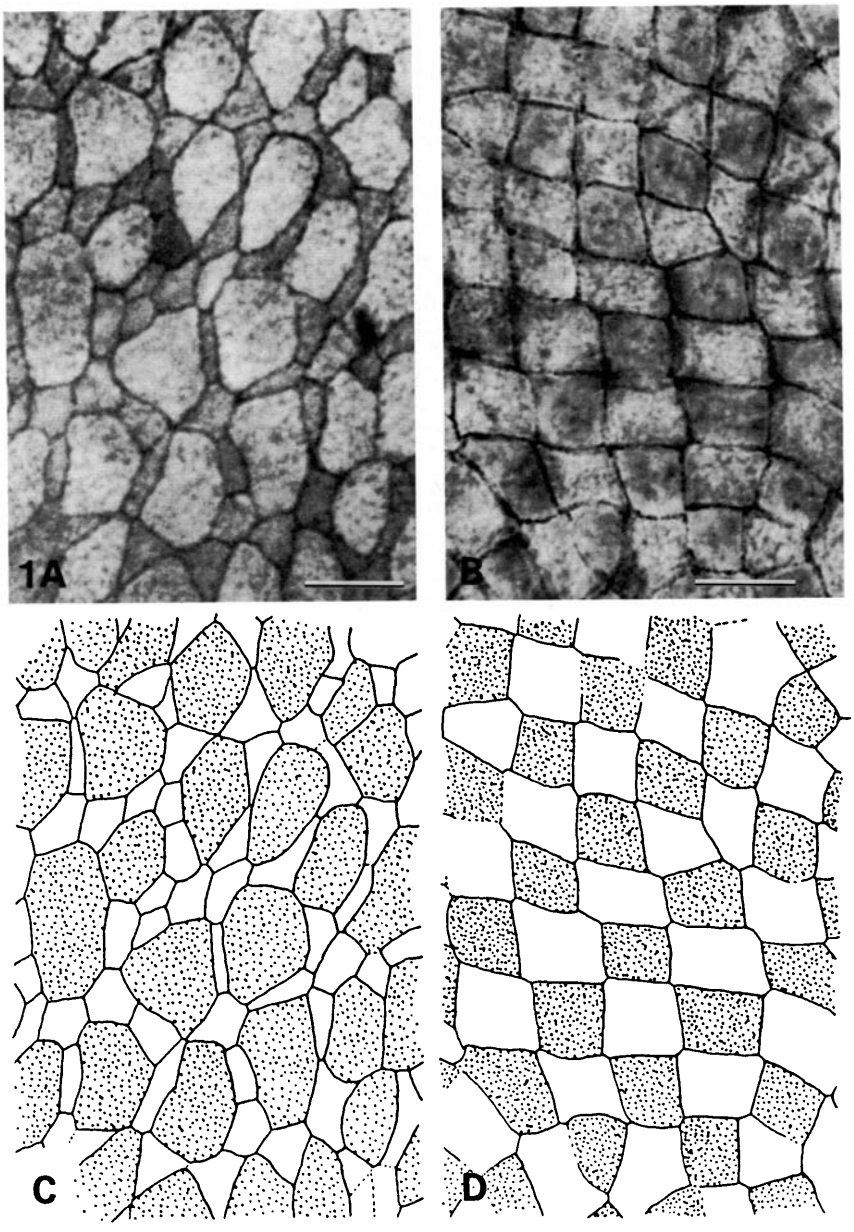

Fig. 1. (A) A luminal surface of an immature oviduct epithelium just before sexual maturation (quail, 41 days after hatching). (B) A luminal surface of a mature oviduct epithelium. A and B were treated with silver nitrate and photographed through an optical microscope. Bar, 10 μm. (C,D) Drawings from A and B indicating C-cells (stippled). C-cells in C are large and surrounded by G-cells (small nonstippled cells). C-cells in D are rectangular, whereas G-cells are generally octagons consisting alternately of small and large sides. Most of the C-cells in D are also surrounded by G-cells.

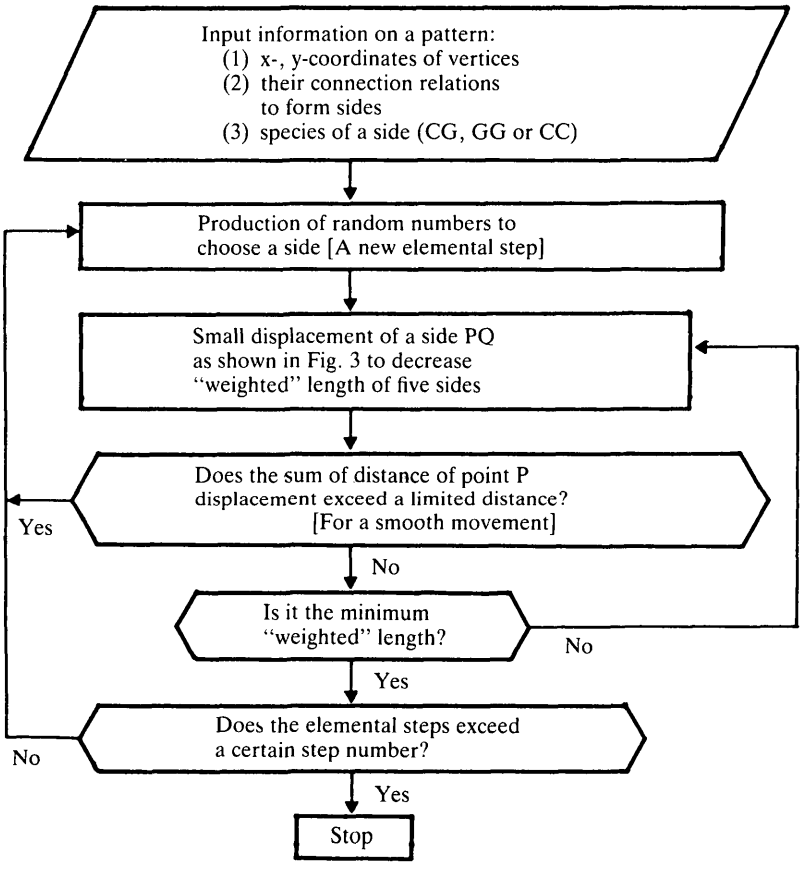

Fig. 2. Standard procedure for the improved boundary shortening.

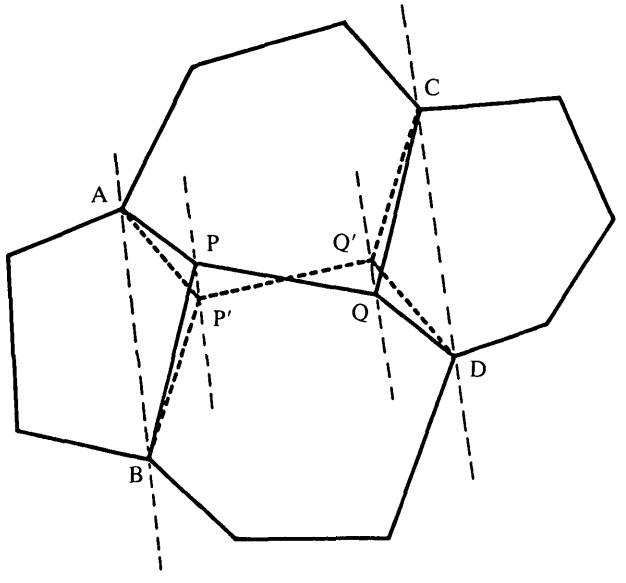

Fig. 3. An elemental step of the boundary shortening procedure. Vertices P and Q linked by a side are moved while keeping a constant area for each domain, so that the total length of five sides (AP′ + BP′ + P′Q′ + Q′C + Q′D) becomes a minimum. PP′ and QQ′ are parallel with AB and CD, respectively. When P moves to P′, Q is forced to move to Q′ so as to keep a constant area for two respective polygons (polygon APQC and polygon BPQD).

and G (gland), in a system, weighting factors are presented by a_{CG}, a_{GG} or a_{CC} which is for CG, GG or CC boundary, respectively. We normalized a_{GG} (= 1·0) without losing generality. The weighting factors were all the same (1·0) in the case of the usual boundary shortening model. P′ was sequentially moved away from P by small distances (positive or negative) so that the weighted length of the five sides internal to the group of four cells becomes smaller.

(2) *For a smooth movement*

In order to realize a smooth movement, the movement of point P was restricted as follows. If the total distance of sequential movements of P in an elemental step was over a given limited distance (for example, 1·0 mm), the P movement ceased. Point P remained there until it was selected again randomly (see Fig. 2). This is the elemental step of the boundary shortening procedure.

All information on a given pattern (x-, y-coordinates of vertices, their connection relation and indication of cell types) was stored on a computer disc. The elemental step of the boundary shortening procedure was performed on a side that was randomly selected. The elemental steps were repeated on several thousand random numbers until the total weighted length of the sides in a polygonal pattern (the total weighted boundary length) ceased to decrease. Thus, we obtained a theoretically predicted pattern after hypothetical shortening of cell boundaries.

Periodic boundary conditions of the rectangle [side length ratio, 2: $\sqrt{3}$; side angle, 90°; point (x,y) is equivalent to ($x \pm 2L$, $y \pm \sqrt{3}L$)] and the rhomboid [4:5; 60°; point (x,y) is equivalent to ($x \pm 5L\cos 60° \pm 4L$, $y \pm 5L\sin 60°$)] were used for computation, where L is a constant concerning pattern size. Calculation and simulation were carried out by an electronic digital computer of Facom OS IV/F4 [E40] (Fujitsu, Co.).

RESULTS

Part I. Two factors that contribute to oviduct cellular patterns of the adult quail

Cell boundary contraction of the oviduct epithelium

The oviduct epithelium is a monolayer sheet of columnar cells, that shows a polygonal pattern on its luminal (apical) surface. Bundles of microfilaments consisting of actin filaments run inside the cells along lateral intercellular boundaries just below the apical surface level (Honda, 1983; Yamanaka & Honda, in preparation). Thus the bundles of microfilaments form polygonal networks just below the apical surface of the oviduct epithelium. The bundles are the same as the circumferential bundles of microfilaments in the retinal pigment epithelial cell which has been demonstrated to have contractility (Owaribe, Kodama & Eguchi, 1981). We expect that a contractile process involving these microfilaments shortens the polygonal cell boundaries in the oviduct epithelium while keeping cell contact between neighbouring cells. The contractile microfilament bundles have been studied in some epithelial sheets: retinal pigment epithelium, lung epithelium, cornea endothelium, etc. (Honda & Eguchi, 1980; Owaribe, Kodama & Eguchi, 1981; Owaribe & Masuda, 1982; Honda, 1983).

Differential adhesion among cells

Pattern formation in a cell aggregate consisting of two types of cells was explained systematically in terms of differential adhesion among cells (e.g. Steinberg, 1963, 1978). Consider a system in which there are two types of cells in an

aggregate. If the intercellular adhesion between unlike cells is weaker than either of the cohesions between like cells, cells of the two types sort out to form two separate aggregates. When the adhesion between unlike cells is stronger, but less than the average strength of cohesions between like cells, cells of the less cohesive type partially or completely engulf a cluster of cells of the more cohesive type. If the adhesion between unlike cells is still stronger, the two types of cells intermix in a single aggregate.

We will consider a two-dimensional cell aggregate, that is the monolayer cell sheet of the oviduct epithelium. The oviduct epithelium consists of two types of cells, ciliated cells (C-cells) that have many cilia on the apical surface and gland cells that secrete ovomucin (G-cell). If we assume the adhesion between C- and G-cells is stronger than cohesion between G- and G-cells or between C- and C-cells, we can understand the formation of checkerboard-like pattern as shown in Fig. 1B,D. Most of the cell boundaries in the pattern are edges along which C- and G-cells meet. The GG and CC boundaries are small or few in number.

A balanced state between two effects, boundary contraction and differential adhesion

Boundary contraction of cells tends to form a honeycomb pattern as shown in Fig. 4A since the boundary length of the honeycomb pattern is minimum. On the other hand, the strong intercellular adhesion between unlike cells tends to form a checkerboard pattern as shown in Fig. 4C since all cell boundaries are between different types of cells. Neither pattern simultaneously meets the demands of both boundary contraction and differential adhesion.

Actual oviduct epithelia show a pattern similar, but not identical, to a checkerboard (Fig. 1B,D, 4B). Most of the polygons look like squares, but, in reality, some of them are octagons including four short sides. That is, there are minor (short) GG or CC boundaries in addition to main (long) CG boundaries in the pattern. The deviation from the checkerboard pattern is considered to be caused by the boundary contraction. The actual cellular pattern of the oviduct epithelium

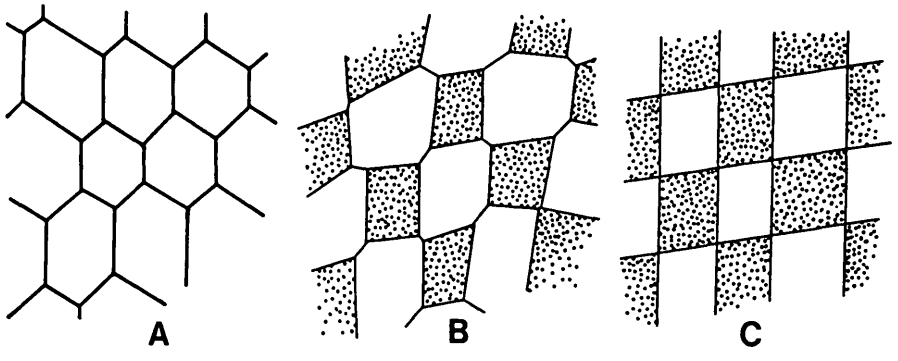

Fig. 4. An actual cellular pattern of the oviduct epithelium (B) is intermediate between two typical artificial patterns, a honeycomb pattern (A) and a checkerboard one (C).

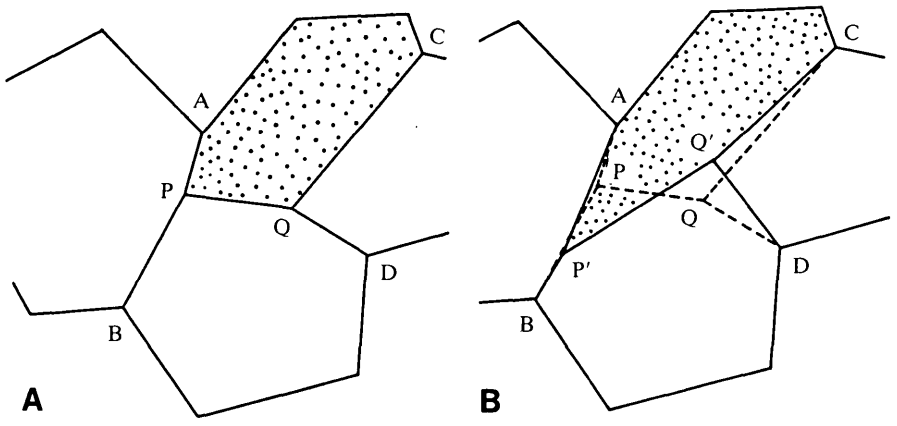

Fig. 5. Elemental steps of the procedure of shortening nonweighted (A) or weighted (B) boundary length. P and Q are movable vertices. One C-cell is designated by stippling. The other three cells are G-cells. Parameter values of weighting factors are as follows: $a_{CG} = a_{GG} = 1{\cdot}0$ in A, and $a_{CG} = 0{\cdot}4$, $a_{GG} = 1{\cdot}0$ in B.

is in a balanced state between the two effects from differential adhesion and from boundary contraction.

Estimation of the difference of intercellular adhesions

In other words, the actual cellular pattern of the oviduct epithelium is considered to be deformed from a honeycomb pattern on account of the stronger intercellular adhesion between unlike cells than between like cells. In order to introduce the effect of differential adhesion into the boundary shortening model of cells, we have modified the previous boundary shortening model as described in Materials and Methods. Here, we use numerical values a_{CG}, a_{GG} or a_{CC} (where a_{GG} has been normalized as 1·0 as described in Materials and Methods) for five weighting factors a_{AP}, a_{BP}, a_{PQ}, a_{QC} and a_{QD} according to the respective species of cell boundaries CG, GG or CC.

An example of boundary shortening in a simple pattern is shown in Fig. 5. Polygon APQC is a C-cell, and all of the other polygons are G-cells. Therefore, we use the value of a_{CG} for a_{AP}, a_{PQ} and a_{QC}, and the value of a_{GG} for a_{BP} and a_{QD}. We perform an elemental step of boundary length shortening by using $a_{CG} = 1{\cdot}0$. A resultant pattern is shown in Fig. 5A; this is the same pattern as obtained with the usual model of Fig. 3. On the other hand, when using $a_{CG} = 0{\cdot}4$ the pattern is deformed as shown in Fig. 5B after the elemental step. (In this instance, we did not constrain the P movement to give a smooth movement as described in Materials and Methods.) The lengths of the CG boundaries (AP′, P′Q′) are greatly elongated and the length of the GG boundary (BP′) is shortened. This is an effect of the strong adhesion between unlike cells along the CG boundaries which is produced using $a_{CG} = 0{\cdot}4$. (Note that a_{CG} is less than a_{GG}.)

We next shorten the weighted boundary length of actual oviduct epithelial patterns such as Fig. 6 using various values of a_{CG} while fixing a_{CC} at 1·0. We will

look for a value of a_{CG} at which a given pattern is scarcely deformed from an original pattern. In order to know the extent of pattern deformation, we used an s-value that is defined as the percentage of decrease in the total (not weighted) boundary length during shortening of the weighted boundary length (Honda & Eguchi, 1980; Honda, 1983). Results are shown in Fig. 7. The s-value is almost zero when $a_{CG} = 0{\cdot}43$. We displayed a resultant pattern on an XY plotter and confirmed that the pattern was not significantly deformed from the original pattern. A similar result was obtained by using another actual pattern of the oviduct epithelium (open and solid circles in Fig. 7).

Part II. A computer simulation of the transformation of the kagome pattern to the checkerboard pattern

The kagome (or star) pattern

An immature oviduct epithelium just before sexual maturation (about 40–45 days after hatching) shows another peculiar pattern in addition to the checkerboard one (Yamanaka, in preparation). The oviduct epithelium at this stage is also a monolayer consisting of columnar C- and G-cells. However, a luminal surface

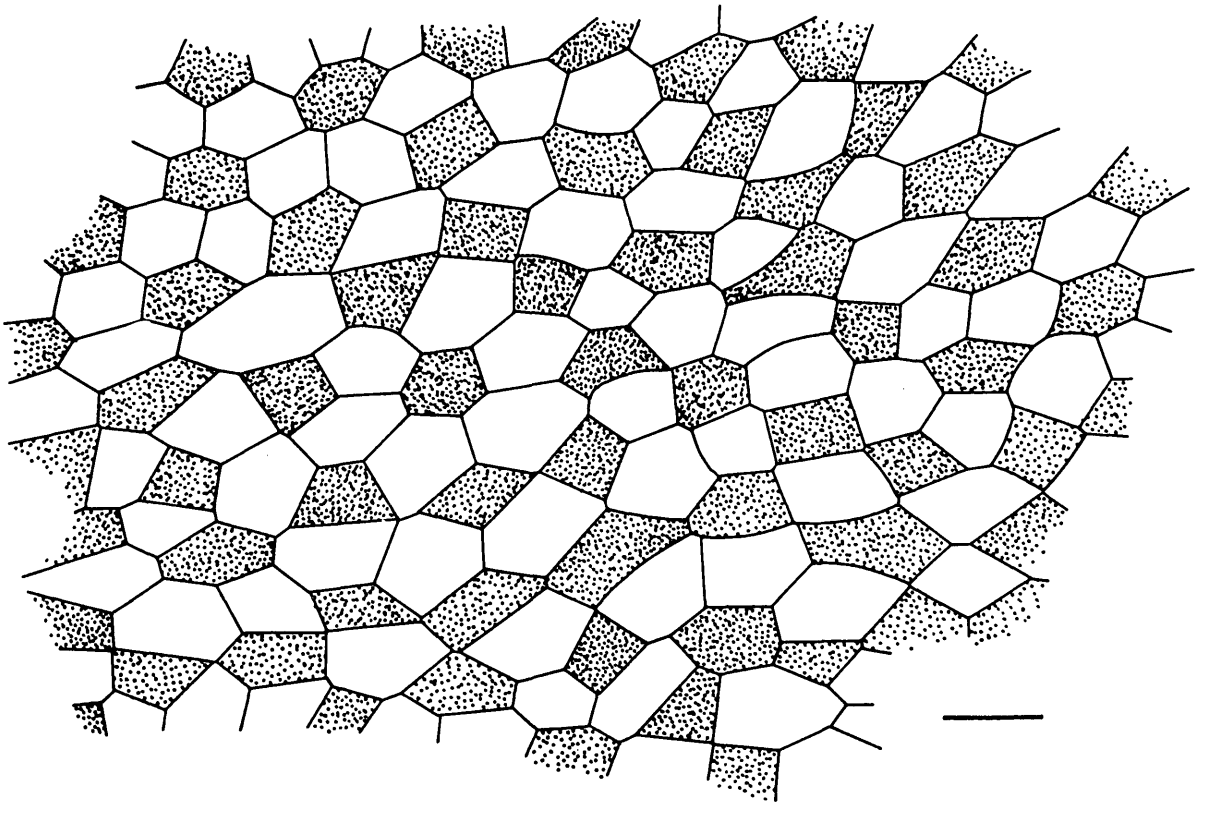

Fig. 6. One of the checkerboard-like patterns found in the oviduct epithelium. The drawing is from a microphotograph of microfilament bundles according to Yamanaka & Honda (in preparation). C-cells are designated by stippling. All other cells are G-cells. Bar, 10 μm.

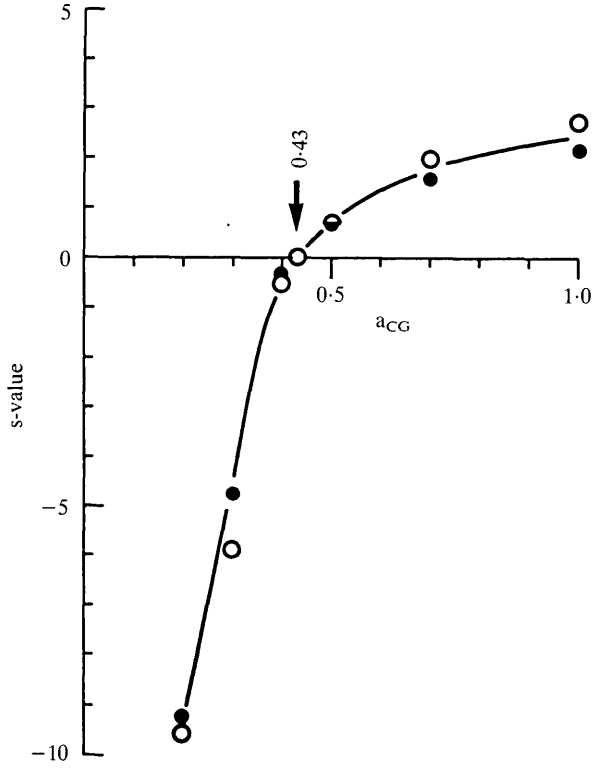

Fig. 7. Estimation of the weighting factor (a_{CG}) value at which actual cell patterns are scarcely deformed during the procedure of shortening the weighted boundary length. a_{CC} and a_{GG} are fixed at 1·0 throughout. The s-value, which is a percentage of a decrease of the total (nonweighted) boundary length during 5000 steps of the procedure, is used to determine how much a pattern is deformed. We obtain $a_{CG} = 0{\cdot}43$ where the s-value is almost zero. We confirm by displaying resultant patterns on an XY plotter that the patterns are not significantly deformed from the original ones when $a_{CG} = 0{\cdot}43$. ○, data obtained by using the pattern of Fig. 6. ●, data from another pattern of the oviduct epithelium.

shows a pattern in which large C-cells are surrounded by small G-cells as shown in Fig. 1A,C. Most of the C-cells do not lie next to each other, whereas all G-cells form chains that enclose isolated C-cells. The arrangement of these cells looks like a 'kagome' pattern, one of the woven patterns appearing in Japanese traditional bamboo ware. Fig. 8 shows the theoretical continuous change of a honeycomb pattern to a kagome pattern. The actual immature oviduct epithelium corresponds to the middle part of Fig. 8 (we will call it a *modified* kagome pattern), in which small cells link together to surround a large cell. The ratio of small cells to large cells in the artificial pattern of Fig. 8 is 2·0, which is close to the cell ratio in an actual immature oviduct epithelium such as Fig. 1A (2·12 = 474/223).

Consideration on the kagome–checkerboard transformation

We next consider the pattern transformation from kagome to checkerboard with respect to cell number and size. The oviduct grows from approximately 12 cm to

18 cm in length during the kagome–checkerboard transformation (Yamanaka, in preparation). Roughly speaking, it increases 1·5-fold in length and then 2·3-fold in surface area. We count cells using photographs such as Fig. 1A and B. At the kagome stage there are 223 C-cells and 474 G-cells in a certain area (20 000 μm^2). At the checkerboard stage there are 407 C-cells and 479 G-cells in an area (20 000 $\mu m^2 \times 2{\cdot}3$) which corresponds to a region of area (20 000 μm^2) at the kagome stage. These numerical data suggest that C-cells divide once during the transformation since 446 (223×2) corresponds to 407 for C-cells and 474 to 479 for G-cells. We can conclude that during the kagome–checkerboard transformation C-cells divide once whereas G-cells do not divide and the luminal surfaces of all cells increase 2·3-fold.

We intend to perform a computer simulation on the transformation to the checkerboard pattern from the modified kagome pattern (the middle part of Fig. 8). Large regular hexagons correspond to C-cells which are going to divide once. Small hexagons consisting of alternate long and short sides correspond to G-cells which surround isolated C-cells.

Determination of the weighting factor a_{CC}

When we determined $a_{CG} = 0{\cdot}43$ we fixed a_{CC} at the value 1·0 arbitrarily. The arbitrary fixation of the a_{CC} value was justified, since there were scarcely any CC boundaries in the actual cellular patterns. However, there are many CC boundaries in the modified kagome pattern in which all C-cells have divided as shown in Fig. 9A. We have to determine a definite value of a_{CC}. We performed the improved boundary shortening procedure, using various a_{CC} values with

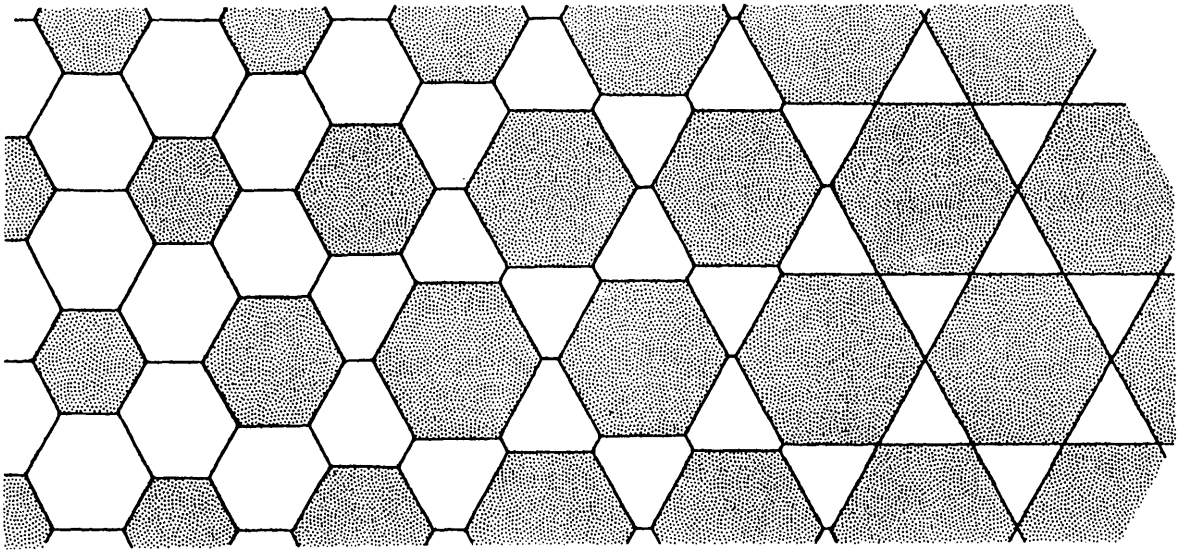

Fig. 8. Change of an artificial pattern from honeycomb (left) to kagome (right). The middle is a modified kagome pattern which corresponds to the typical cellular pattern of avian oviduct just before sexual maturation. Hexagons corresponding to C-cells are designated by stippling.

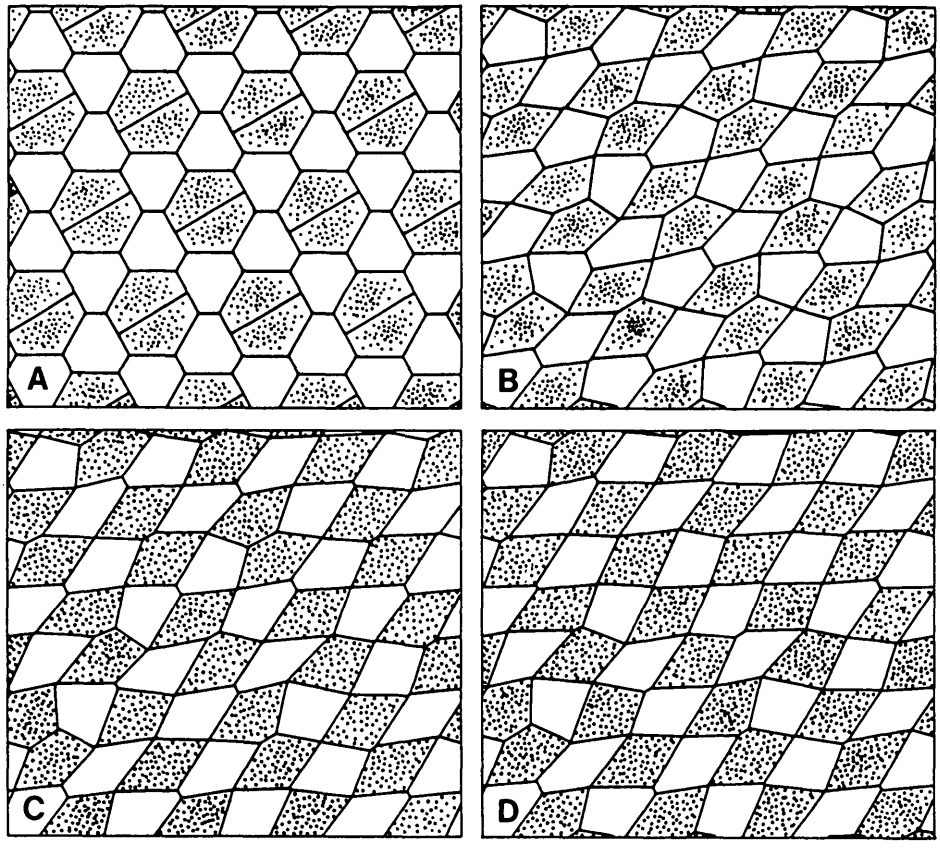

Fig. 9. A computer simulation of the transformation starting with a modified kagome pattern. (A) A modified kagome pattern where C-cells (stippled polygons) divide in parallel with each other. All polygons are the same in area. The procedure of shortening the weighted boundary length is performed on the pattern A, putting $a_{CG} = 0{\cdot}43$, $a_{GG} = 1{\cdot}0$ and $a_{CC} = 1{\cdot}8$. A rectangular cyclic boundary condition is used. (B) After 2000 steps. (C) After 9000 steps. (D) After 40 000 steps. The pattern comes to resemble a checkerboard.

$a_{CG} = 0{\cdot}43$, on the modified kagome pattern in which C-cells divided. When $a_{CC} = 1{\cdot}0$ or $1{\cdot}5$, all cells in the pattern are deformed into pentagons. When $a_{CC} = 1{\cdot}8$ or $2{\cdot}0$, the cellular pattern somewhat resembles a checkerboard; when $a_{CC} = 2{\cdot}5$, the pattern shows many singular figures despite the constraint that the P movement should be smooth. (See Fig. 13A which will be discussed later.) We will then use $a_{CC} = 1{\cdot}8$ hereafter for the computer simulation of the pattern that includes many CC boundaries. Interpretations of the a_{CC} value will be discussed later.

Computer simulations of the kagome–checkerboard pattern transformation

A computer simulation of the pattern transformation started with the modified kagome pattern shown in Fig. 9A. The area of C-cells (large regular hexagons) was assumed to be twice that of G-cells (small hexagons) in a luminal surface and

the cleavage planes for all C-cells were parallel to each other. The improved boundary shortening procedure was performed on the pattern of Fig. 9A using $a_{CG} = 0{\cdot}43$, $a_{GG} = 1{\cdot}0$ and $a_{CC} = 1{\cdot}8$. A rectangular cyclic boundary condition was used. The resultant patterns after 2000, 9000 and 40 000 steps are shown in Fig. 9B,C,D, respectively. Fig. 9D shows a pattern resembling a checkerboard; most of the boundaries are edges along which C- and G-cells meet.

Similar results, as shown in Fig. 10A,B, were obtained by using a different series of random numbers which determined other sequences of selecting sides in the boundary shortening procedure. The resultant pattern in the case of a rhomboidal cyclic boundary condition is also shown in Fig. 10C which is similar to other results (Figs 9D, 10A,B). Fig. 9A corresponds to an actual pattern of Fig. 1A,C. Figs 9D and 10A–C should be compared with an actual pattern of Fig. 1B,D.

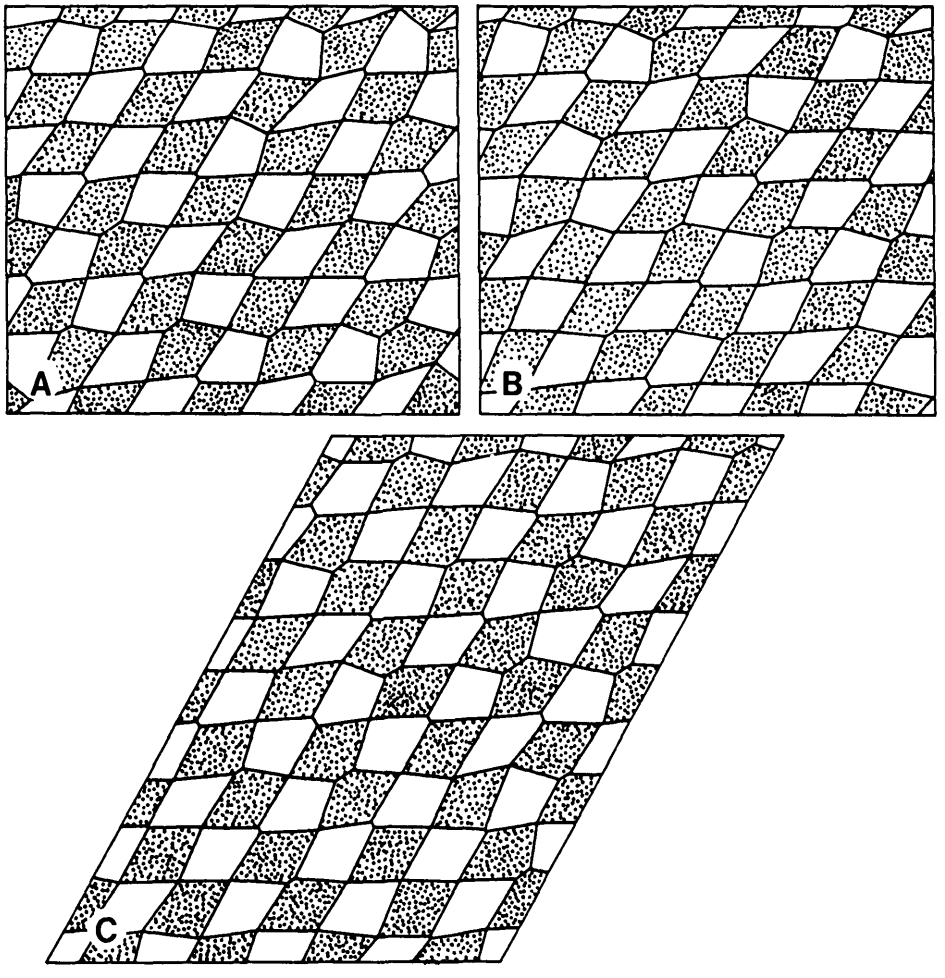

Fig. 10. As in Fig. 9; results of computer simulations under different conditions. (A) Using other series of random numbers than in Fig. 9. After 9000 steps. (B) Using other series of random numbers than those in Figs 9, 10A. After 4000 steps. (C) Using a different cyclic boundary condition (a rhomboid). After 40 000 steps.

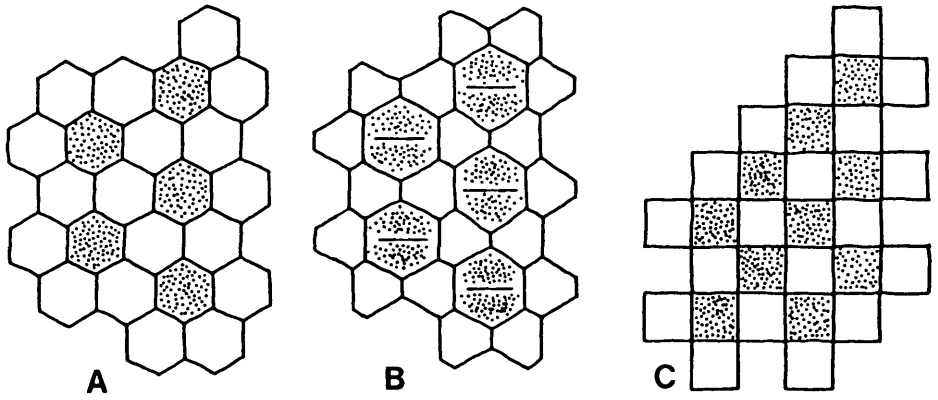

Fig. 11. Schematic cellular pattern change during sexual maturation of the avian oviduct epithelium. Stippled polygons are C-cells. Others are G-cells. (A) Maximal dispersion of C-cells among G-cells, using the condition that C-cells do not adjoin each other. Thus, there is no CC boundary. The ratio of C-cells to G-cells is 1/2. (B) C-cells enlarge their area relative to G-cells so as to decrease the length of GG boundaries, thus forming a modified kagome pattern. Next, CC boundaries are generated through divisions of C-cells. (C) A checkerboard pattern forms so as to decrease CC boundaries. Thus, all boundaries are edges along which C- and G-cells meet.

DISCUSSION

The developmental process of the oviduct epithelium

A sequence of cellular pattern changes has been observed in oviduct epithelium of the Japanese quail (Yamanaka, in preparation). The epithelium just after hatching consists of undifferentiated cells of a single type which form a monolayer cell sheet. In luminal surface view cells in the monolayer have sinuous boundaries that form a pattern resembling a jigsaw puzzle. This pattern lasts until about 32 days after hatching. During the next stage (approximately from 32 to 40 days) the cell boundaries change from sinuous to straight and cells form polygons. The cells differentiate into C- or G-cells and vary in size. There are fewer C-cells than G-cells. This pattern is called *random polygons*. G-cells have a tendency to link with each other, whereas C-cells have a tendency not to contact each other. Finally G-cells form chains that enclose an isolated C-cell; that is, the kagome pattern forms as described already.

We are interested in the patterns of only the luminal surface of the epithelium. The patterns are considered to form and transform mainly due to lateral relationships between neighbouring cells. We have omitted the basal relationship with basement membrane, because the oviduct epithelial cells are columnar and so tall (Yamanaka, in preparation) that adhesion of the cell bottom to the basement membrane is considered not to affect significantly the behaviour of the apical part of a cell. The distance of cell displacement during the computer simulation is small in comparison with the cell height.

The purpose of the present investigation has been to explain theoretically the pattern transformation from kagome to checkerboard (Fig. 11B–C). We have

shown that two factors, the boundary shortening properties and the stronger adhesion between C- and G-cells than between two C-cells or two G-cells, are *sufficient* to explain the pattern transformation using computer simulations. But it should be noted that we cannot say these two factors are *necessary* for the pattern transformation. We cannot exclude other possible mechanisms to explain the pattern transformation. This is the limitation of computer simulation studies.

We now discuss some assumptions we have made in the present computer simulation.

The kagome pattern

We first discuss the geometrical configuration of the kagome pattern. For simplicity we will use a hexagonal pattern as a typical polygonal pattern. Consider a polygonal pattern in which all polygons are G-cells. The problem is to distribute as many as possible C-cells among G-cells with the condition that C-cells do not adjoin each other. One solution is the pattern shown in Fig. 11A. The ratio of C-cells to G-cells in the pattern is 0·5, which is the maximum possible value among solution patterns, and close to the value of an actual kagome pattern (0·47 = 223/474) as already described in Part II of Results. (There are two possible mechanisms forming this pattern in the developmental process: (1) immature cells differentiate into C-cells spontaneously, but, when they adjoin C-cells, they differentiate into G-cells; and (2) a cell divides at or migrates to a boundary where two C-cells adjoin and differentiates into a G-cell.) A similar idea has been discussed with respect to the distribution of ciliated cells on the epidermis of an axolotl embryo (Landström, 1977). It seems that ciliated cells in some epithelial tissues are prohibited from directly contacting each other. After the arrangement of cells as shown in Fig. 11A, the C-cells of the oviduct epithelium enlarge its luminal area to form the kagome pattern as shown in Fig. 11B, at the same time as the length of GG boundaries decreases in the pattern.

It should be noted that, in contrast to the checkerboard pattern, the typical kagome pattern simultaneously meets both demands of (1) the large cell boundaries between unlike cells and (2) the boundary contraction. All cell boundaries in the kagome pattern (the right part of Fig. 8) are between unlike cells where the C- and G-cells meet and its total boundary length is minimal. The minimum boundary length can be inferred as follows. Triangles in the kagome pattern in the right part of Fig. 8 are considered to be the extreme case of small hexagons in the middle of Fig. 8 whose three minor sides shorten and finally disappear. Not only the large polygons (regular hexagons), but also the small polygons in a modified kagome pattern are hexagonal; their inner angles are all 120°. A theorem of geometry states that a hexagonal pattern whose inner angles are all 120° has the minimum boundary length, even if the side lengths are heterogeneous. Therefore, the total boundary length is the same among various patterns in Fig. 8 and its value is minimal.

The direction of cell division

We have assumed that all C-cells divide in the same direction. We will explain in this section that this assumption seems to be reasonable.

Hofmeister (quoted in Korn & Spalding, 1973) observed that a cell divides perpendicular to its long axis. We have confirmed this fact in the epithelium of the starfish embryo (Honda, Yamanaka & Dan-Sohkawa, 1984).

Next, a method to determine the long axis of a cell has been developed and successfully used for the computer simulation of cell divisions (Honda *et al.* 1984). That is, a cell is considered as a polygon made from thin uniform board. The polygonal board has a moment of inertia. We can determine three mutually perpendicular axes through the centre of mass of the polygonal board according to elementary mechanics, so that the moment of inertia about one of these axes has the minimum possible value for any axis through the centre of mass. Then, we used the axis of the minimum value as the long axis of a polygon. Therefore, we can determine a division plane when the shape of a polygonal cell is given.

A C-cell (a regular hexagon) in the modified kagome pattern divides. One of the modes of division is shown in Fig. 12A. The improved boundary shortening procedure is performed on Fig. 12A. The resultant pattern is shown in Fig. 12B. Polygons around the divided cell are somewhat deformed. Directions of long axes of six deformed large hexagons are determined by the method of the moment of inertia as described above and the division planes that are perpendicular to the long axes are determined as shown in Fig. 12B. Four out of six hexagons (solid

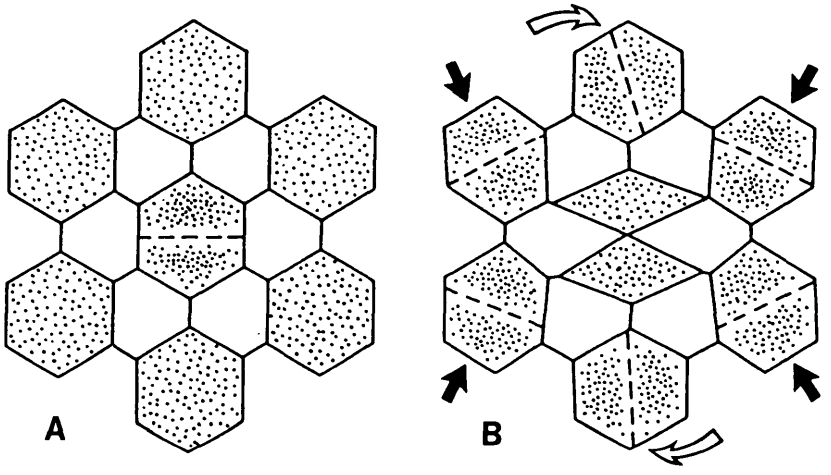

Fig. 12. The effect of a single C-cell division on the adjacent six C-cells. C-cells are designated by stippling. (A) Before cell division. Direction of a cell division is indicated by a broken line. (B) A computer simulation of a polygonal pattern after division with 9000 steps using $a_{CG} = 0{\cdot}43$, $a_{GG} = 1{\cdot}0$ and $a_{CC} = 1{\cdot}8$. Six C-cells around the divided cell are deformed and directions of the next division are determined according to the assumption that a cell divides perpendicular to its long axis. Four cells (solid arrows) that are greatly deformed divide almost in parallel with the initial division. Two cells (open arrows) that are slightly deformed divide approximately perpendicular to the initial division.

arrows in Fig. 12B) suffer relatively large deformations and their division planes are almost in parallel with the division plane of the central polygon which previously divided. The remaining two hexagons (open arrows in Fig. 12B) deform slightly and their division planes are approximately perpendicular to the division plane of the central polygon. Similar results are obtained using a number of procedures with modes of cell divisions other than Fig. 12A.

Based on the information obtained from the above-mentioned computer simulation of a single C-cell division (Fig. 12), consideration proceeds as follows. When a C-cell divides in the modified kagome pattern, four of six cells close to the divided cell are greatly deformed and begin to divide in parallel with the first division. Thereafter, most of the other C-cells around the site are deformed and divide sequentially in parallel with the first division. On the other hand, the remaining two cells close to the original dividing cell are slightly deformed and have a slight tendency to divide perpendicular to the first division, but the tendency is disturbed by many neighbouring cells dividing in parallel with the first division. Therefore, we have reasonably postulated that C-cells in the modified kagome pattern divide in parallel with each other in a restricted area. We await further studies that show cell divisions of the same direction in actual tissues.

The effect of the smooth movement of point P

As described in Materials and Methods, the movement of point P is restricted within a given distance during a single elemental step in the present investigation. We suggest that the restriction causes point P to move in a natural, reasonable manner, since actual movements of cell boundaries in a tissue take place simultaneously in many locations, while cell boundaries in a computer simulation move one by one. It is far from natural that, while a certain cell boundary moves greatly, other cell boundaries do not move at that time. Although there is a restriction of P movement during a single elemental step, many repetitions of these elemental steps result in many small movements of vertices in several locations, which is close to actual cell behaviour. In comparison with the conventional computation more steps are necessary to get the pattern change. When the computer simulation runs without the restriction of P movement, the resultant patterns often contain singular figures as shown in Fig. 13A. In contrast, we obtain reasonable figures as shown in Fig. 13B by using the program to restrict the movement of P. The assumption of the smooth P movement has therefore been used in the present computer simulation.

Meanings of the values a_{CG} and a_{CC}

An interpretation of $a_{CG} = 0{\cdot}43$ is as follows. Shortening of the cell boundaries is considered to contribute to stabilization of the epithelium. In the oviduct epithelium, moreover, the decrease of a unit length of GG boundary contributes to the stabilization more than the decrease of a unit length of CG boundary. The length of GG boundary then tends to become short in comparison with the length of CG boundary. Quantitatively, the decrease of 2·33 ($= 1/0{\cdot}43$) of CG boundary

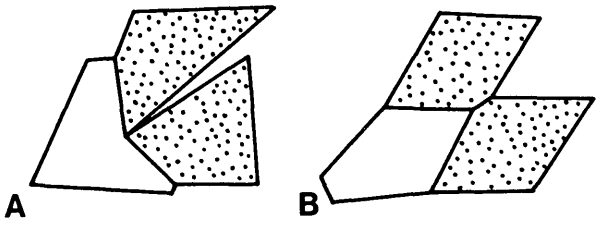

Fig. 13. The effect of the smooth movement of point P. The improved boundary shortening procedure without the restriction of the P movement sometimes generates a singular pattern such as A. When restricting the P movement during a single elemental step (see Materials and Methods), a regular pattern such as B is obtained. C-cells are designated by stippling.

length makes the same contribution as the decrease of a unit of GG boundary length. We cannot define the physical meanings of $a_{CG} = 0{\cdot}43$ more precisely, but the present interpretation seems to be important since we do not have any other method to obtain quantitative information on the adhesion strength of cells being organized into tissues *in situ*.

We have used $a_{CC} = 1{\cdot}8$, but the value is not as reliable as the value of a_{CG} when considering the process of determination of the a_{CC} value. We can say, however, it is meaningful that the value of a_{CC} is considerably larger than that of a_{GG} ($= 1{\cdot}0$) because the frequencies of CC boundaries are few in comparison with those of GG boundaries in the oviduct epithelium (Yamanaka & Honda, in preparation). That is, C-cells have a tendency not to contact each other whereas G-cells link with each other.

Rhombic checkerboard pattern

Our computer simulation of the transformation from the modified kagome pattern results not in orthogonal, but rhombic checkerboard patterns as shown in Fig. 9D, 10. This is not due to the shape of a cyclic boundary condition, since the different cyclic boundary conditions of rectangle (Fig. 9D, 10A,B) and rhomboid (Fig. 10C) have both given similar results. Cells in the modified kagome pattern correspond one-to-one to cells in the resultant checkerboard pattern as shown in Fig. 14. Averaged positions of individual cells have not shifted significantly during computer simulation. This is why we do not get orthogonal cell arrays. Cells would have to be moved for a long distance in order to obtain an orthogonal checkerboard pattern in a computer simulation. Pattern changes not involving long-distance cell shifts are due to the limited ability of side movements in the boundary shortening procedure, that is sides of polygons move one by one keeping constant polygonal areas.

Functions of the checkerboard-like arrangement of cells

The checkerboard-like cell arrangement makes an even distribution of C-cells and G-cells on the luminal surface of the oviduct. Cilia movement of C-cells and

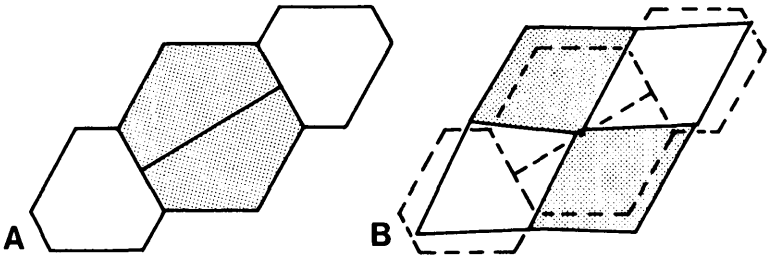

Fig. 14. Correspondence of initial polygons (A) to the final ones (B) in a computer simulation of the pattern formation. Polygons do not shift significantly during the simulation. The resultant polygons are not squares, but have been deformed into rhomboids. C-cells are designated by stippling.

ovomucin secretion from G-cells both help the transport of an egg through an oviduct tube. Therefore, the even distribution of C- and G-cells is considered to promote egg transport.

We have observed coated pit-like structures on a lateral boundary between two columnar cells in the oviduct epithelium with an electron microscope (unpublished results). This might suggest a transportation of substances between the two types of cells. We are not sure whether the effective transport of certain substances across CG boundaries is required for cell survival. If it is, then cell configurations like a checkerboard and kagome are adaptive for effective transport, since both configurations provide large lateral boundaries between unlike cells. A similar discussion has taken place with regard to counter-current exchange within a bundle of small blood vessels (veins and arteries) in the wall of the swimbladder of deep-sea fishes (Scholander, 1969).

In the differential adhesion theory of cell aggregates (e.g. Steinberg, 1963, 1978), the intermixing case has only been theoretical: there has been no actual case in which two types of cells mix with each other and do not sort out. Our finding of the checkerboard pattern in the avian oviduct epithelium may be the first instance. However, our instance is in a two-dimensional cell aggregate, not in a three-dimensional one.

We thank Dr Jay E. Mittenthal (University of Illinois, Urbana, USA) for critical reading of the manuscript, Dr Tadashi Oishi (Nara Women's University, Nara, Japan) and Dr Ryuji Kodama (National Institute for Basic Biology, Okazaki, Japan) for encouragement, and Ms Yoshiko Tanaka-Ohmura and Ms Akemi Hayashi (Kanebo Institute) for their skilful assistance in microscopy. We also thank an anonymous reviewer for help in improving the manuscript. The present investigation is supported in part by grants to G.E. in aid for Special Project Research, General Research and Cancer Research from the Japan Ministry of Education, Science and Culture.

Part of the present investigation has been presented in The First International Symposium for Science on Form in Tsukuba, Japan (26–30 November 1985).

REFERENCES

HONDA, H. (1983). Geometrical models for cells in tissues. *Int. Rev. Cytol.* **81**, 191–243.

HONDA, H., DAN-SOHKAWA, M. & WATANABE, K. (1983). Geometrical analysis of cells becoming organized into a tensile sheet, the blastular wall, in the starfish. *Differentiation* **25**, 16–22.

HONDA, H. & EGUCHI, G. (1980). How much does the cell boundary contract in a monolayered cell sheet? *J. theor. Biol.* **84**, 575–588.

HONDA, H., OGITA, Y., HIGUCHI, S. & KANI, K. (1982). Cell movements in a living mammalian tissue: long-term observation of individual cells in wounded corneal endothelia of cats. *J. Morph.* **174**, 25–39.

HONDA, H., YAMANAKA, H. & DAN-SOHKAWA, M. (1984). A computer simulation of geometrical configurations during cell division. *J. theor. Biol.* **106**, 423–435.

KORN, R. W. & SPALDING, R. M. (1973). The geometry of plant epidermal cells. *New Phytol.* **72**, 1357–1365.

LANDSTRÖM, U. (1977). On the differentiation of prospective ectoderm to a ciliated cell pattern in embryos of *Ambystoma mexicanum*. *J. Embryol. exp. Morph.* **41**, 23–32.

OWARIBE, K., KODAMA, R. & EGUCHI, G. (1981). Demonstration of contractility of circumferential actin bundles and its morphogenetic significance in pigmented epithelium *in vitro* and *in vivo*. *J. Cell Biol.* **90**, 507–514.

OWARIBE, K. & MASUDA, J. (1982). Isolation and characterization of circumferential microfilament bundles from retinal pigmented epithelial cells. *J. Cell Biol.* **95**, 310–315.

SCHOLANDER, P. F. (1969). In *Vertebrate Structures and Functions* (ed. N. K. Wessells), pp. 125–131. San Francisco: Freeman.

STEINBERG, M. S. (1963). Reconstruction of tissues by dissociated cells. *Science* **141**, 401–408.

STEINBERG, M. S. (1978). Cell–cell recognition in multicellular assembly: Levels of specificity. In *Cell–Cell Recognition. Symp. Soc. Exp. Biol.*, no. **32** (ed. A. Curtis). Cambridge: Cambridge University Press.

(*Accepted 1 July 1986*)